Cancer Nanotechnology

RESEARCH Open Access

Inhibition of malate dehydrogenase via nanoselenium coupling with nanocellulose composite in MCF-7 breast carcinoma cells

Mostafa M. El-Sheekh[1*], El-Refaie Kenawy[2], Wesam E. Yousuf[3] and Tarek M. Mohamed[3]

*Correspondence: mostafaelsheikh@science.tanta.edu.eg

[1] Botany Department, Faculty of Science, Tanta University, Tanta 31527, Egypt
[2] Polymer Research Group Chemistry Department, Faculty of Science, Tanta University, Tanta 31527, Egypt
[3] Biochemistry Division, Chemistry Department, Faculty of Science, Tanta University, Tanta 31527, Egypt

Abstract

Background: Cancer, a leading cause of mortality worldwide, continues to pose significant challenges in treatment and management. Conventional therapies often face limitations, including lack of selectivity, adverse effects, and the development of resistance mechanisms.

Methods: Therefore, this study aims to investigate nanocellulose, nanoselenium, and their nanocomposite which are previously synthesized and characterized. Molecular docking simulations were performed to assess binding affinity to malate dehydrogenase-1 (MDH-1), a key metabolic enzyme in cancer cells. Cytotoxicity was evaluated in A549 lung cancer cell line, the MCF-7 breast cancer cell line, and the WI-38 normal cell line. Mechanistic studies included assessment of MDH-1 activity and expression, intracellular reactive oxygen species (ROS) levels, and cell cycle analysis.

Results: Molecular docking simulations demonstrated a favorable binding affinity (136.98 kcal/mol) of cellulose and selenium as cofactor to the nicotinamide adenine dinucleotide (NAD) + hydrogen (H) (NADH) binding domain of human MDH-1. The nanocomposite exhibited a synergistic impact against cancer, causing a considerable decrease in the viability of MCF-7 cells compared to separate treatments with nanocellulose and nanoselenium. Moreover, it showed negligible toxicity towards normal cells. Biochemical studies demonstrated that nanocellulose, nanoselenium and the nanocomposite substantially reduced MDH-1 activity and messenger ribonucleic acid (mRNA) expression in MCF-7 cells. This was confirmed by flow cytometric analysis, which revealed that the nanocomposite could effectively reduce the intracellular ROS levels and induce potent cell cycle arrest in the G0/G1 phase, that inhibit MCF-7 cell proliferation.

Conclusions: In conclusion, our finding elucidated the promising therapeutic potential of nanocellulose, nanoselenium, and their nanocomposite as effective anticancer agents in breast cancer treatment, demanding further preclinical and clinical investigations to explain their mechanisms of action.

Keywords: Malate dehydrogenase-1, Nanocellulose, Nanoselenium, Nanocomposite, Oxidative stress and cancer

Introduction

Breast cancer is a major health issue that affects many women globally (Arnold et al. 2022). It occurs when cells in the breast grow abnormally and out of control (Maurya et al. 2023). Different types of breast cancer exist and can vary in their behavior and response to treatment (Akram et al. 2017; Iqbal et al. 2022). While early detection and newer targeted therapies have improved outcomes, breast cancer remains a significant challenge (Zhong et al. 2021; Wang et al. 2023). To better understand what causes breast cancer and to come up with better ways to stop, diagnose, and treat it, more study is needed (Britt et al. 2020). There is a need for a targeted and biocompatible alternative to traditional chemotherapeutic medications, which is highlighted by their significant adverse effects and non-specific systemic distribution (Maghsoudnia et al. 2020).

Malate dehydrogenase (MDH) is a metabolic enzyme that is essential in the synthesis of energy where MDH acts as a part of the malate-aspartate shuttle, catalyzes the reversible reaction of oxaloacetate to malate in the presence of NADH and studies have shown that breast cancer cells frequently exhibit higher levels of MDH relative to normal cells (Peng et al. 2022). MDH is a crucial factor in the metabolic reprogramming of cancer cells, namely in the Warburg effect. This effect is characterized by enhanced glycolysis and inhibited oxidative phosphorylation (de Bari and Atlante 2018). The malate-aspartate shuttle facilitates the transport of NADH molecules into mitochondria, while the MDH enzyme aids in the conversion of malate to oxaloacetate. This conversion establishes a connection between glycolysis and the citric acid cycle (Koju et al. 2022). This redox regulation by MDH helps maintain the balance between oxidative and reductive processes, which is crucial for cancer cell proliferation and survival (Eniafe and Jiang 2021). The altered expression and activity of MDH contribute to the metabolic adaptations that support tumor growth, making it a potential therapeutic target (Biancur and Kimmelman 2018).

The field of nanotechnology has shown significant potential in the realm of cancer treatment (Fan et al. 2024) especially green synthesis of nanoparticles (Wang et al. 2024). Nanoscale materials possess distinctive physicochemical features that enable them to engage with biological systems on a molecular scale (Sinha et al. 2022). The therapeutic efficacy and safety of nanotechnology-enabled technologies have been found to be quite promising in this field of cancer (Chuang et al. 2022). One of the most prevalent and renewable biopolymers in the world is cellulose (Li et al. 2021). The utilization of nanocellulose generated from plant sources in biomedical applications is advantageous due to its environmentally friendly nature, as it is biodegradable and exhibits minimal toxicity (Reshmy et al. 2021). The pore nature and extensive surface area of cellulose nanocrystals allow for significant anticancer medication loading (Grishkewich et al. 2017). The anticancer properties of cellulose nanocrystals have been proven both in laboratory experiments (in vitro) and in living organisms (in vivo). These properties are achieved by triggering programmed cell death (apoptosis) and preventing the creation and spread of tumors (metastasis) (Yusefi et al. 2022). Nevertheless, the clinical application of cellulose nanocrystals in cancer therapy has been hindered by several challenges, including inadequate water dispersion and restricted drug loading capacity (Khalil et al. 2023).

Selenium, a dietary micronutrient, has garnered attention due to its antioxidant, antibacterial, and anticancer characteristics (Pandey et al. 2021). When compared to its bulk equivalent, elemental selenium at the nanoscale (nanoselenium) exhibits improved bioavailability and potency (Pandey et al. 2021). Nanoselenium promotes apoptosis, the cell cycle comes to a stop and angiogenesis disruption in tumors (Abd-Rabou et al. 2019). Nevertheless, the clinical utility of nanoselenium is restricted because of its inadequate colloidal stability and vulnerability to agglomeration (Zambonino et al. 2023). The combination of nanoselenium with cellulose nanocrystals promises to solve the natural limitations associated with each constituent.

However, research on nanocellulose–nanoselenium composites for breast cancer therapy is still in the early stages. There is a chance that cellulose-selenium nanocomposites will demonstrate complementary anticancer properties. The cellulose matrix can stabilize the nanoselenium particles and allow for the prolonged release of medication (Zhang et al. 2021). Nanoselenium can enhance the therapeutic potency and share added functionality like antiangiogenic actions to the nanocomposites (Sk et al. 2022). The current study aims to advance the development of new targeted nanomedicines for breast cancer treatment by investigating the cytotoxic effects of nanocellulose, nanoselenium, and their nanocomposite on the MCF-7 breast cancer cell line. Our research stands out through its inclusive approach, surrounding cytotoxicity assessments, molecular docking simulations, gene expression analysis, reactive oxygen species (ROS) modulation studies, and cell cycle affect evaluations. This investigation provides a thorough description of the nanocomposite potential as an anticancer therapy, offering unique insights into its efficacy against breast cancer cells. By combining these diverse analytical techniques, our study delivers a rounded acceptance of how these nanomaterials interact with and affect cancer cells, potentially actually the way for more effective and targeted breast cancer treatments.

Materials and methods

Materials

Nicotinamide adenine dinucleotide (NAD^+) and sodium malate were obtained from Sigma-Aldrich Co. USA. ROS-ID total ROS detection kit (ENZ-51011) was purchased from Enzo Life Sciences, Inc. (Farmingdale, USA). Penicillin–streptomycin solution and fetal bovine serum was obtained from Abcam, USA. Dimethyl sulfoxide (DMSO) was purchased from El-Gomhouria chemicals company, Egypt.

Cultivation of *Ulva lactuca*

The *Ulva lactuca* was collected from the Mediterranean Sea near Alexandria, Egypt, during the spring season. The seaweed is washed with natural seawater and then grown in tanks with continuously running saltwater that has been filtered. The tanks are exposed to 16 h of sunshine and 8 h of darkness. No supplementary nutrition is included. The salinity ranges from 36 to 39 PSU (Practical Salinity Units), while the temperature often falls between 18 and 22 °C throughout the spring season. Variations in salinity and temperature occur naturally, influenced by place of origin and seasonal changes (Wahlström et al. 2020).

Cellulose extraction, synthesis and characterization of nanocellulose, nanoselenium and nanocomposite

The process of separating cellulose from the harvested *Ulva lactuca* seaweed involved several steps. First, the collected seaweed biomass underwent pretreatment procedures to remove impurities and facilitate the subsequent extraction process. Then, a series of chemical treatments were applied to isolate the cellulose component from the other components present in the seaweed, such as hemicellulose, lignin, and other organic compounds. After the cellulose extraction was completed, the recovered cellulose fraction was subjected to various characterization techniques as mentioned by El-Sheekh et al. (2023).

Synthesis and characterization of nanoparticles

Successfully extracting cellulose from *Ulva lactuca*, then nanocellulose is synthesized from it using concentrated sulfuric acid. The synthesis of nanoselenium with the assistance of L-arginine was created by vigorously swirling them together using a magnetic stirrer. Subsequently, a solution of ascorbic acid was added as a gentle reducing agent, causing the previously clear mixture to change color to red which indicates the formation of nanoselenium. After that, their nanocomposite was synthesized by hydrothermal treatment. Our obtained nanoparticles were characterized in our previous paper using techniques including Fourier-transform infrared spectroscopy, X-ray powder diffraction, thermo gravimetric analysis (TGA), scanning electron microscopic (SEM), energy-dispersive X-ray analysis (EDX), transmission electron microscopic (TEM), zeta potential and dynamic light scattering (DLS) (El-Sheekh et al. 2024).

Antitumor efficiency

In vitro cultivation of cells

The Center of Excellence for Research in Regenerative Medicine and its Applications (CERMA) at Alexandria University, Egypt, obtained the breast cancer (MCF-7 #ATCC) cell line, lung cell line (A549 # ATCC CRM-CCL-185), and normal cell line (WISH # ATCC CCL-38) in the American Type Culture Collection organization. The cells stayed cultivated in Dulbecco's Modified Eagle's Medium through 10% fetal bovine serum (FBS), 100 U/mL penicillin, and 100 µg/mL streptomycin. The cells stayed maintained in a humid atmosphere with 5% CO_2 at a temperature of 37 °C (Mukherjee et al. 2023).

MTT assay

The inhibitory effects of cellulose, nanocellulose, selenium, nanoselenium, their nanocomposite, and the standard anticancer drug Dox (doxorubicin) on the growth of A549 lung cancer cells, MCF-7 breast cancer cells, and WI-38 normal cells were evaluated using the MTT assay (Molecular probe, Eugene, Oregon, USA; Cat.no. V-13154) as pronounced by Chen et al. (2023). Cells were placed in 96-well plates at a concentration of 1×10^4 cells per well and left to incubate for 24 h to facilitate adhesion. The cells were subsequently exposed to different quantities of nanocellulose, nanoselenium, nanocomposite, and Dox for 48 h. Cells that were not treated were used as the control. After the specified incubation periods, the culture media was collected, and 100 µL of MTT solution (0.5 mg/mL in PBS) was added to each well. The plates

were incubated at a temperature of 37 °C for 4 h to promote the formation of formazan crystals. The formazan crystals were dissolved in 100 µL of dimethyl sulfoxide (DMSO) by adding it to the solution, and the absorbance was measured at 570 nm using an ELISA reader (StatFax-2100, Awareness Technology, Inc., USA). The mean optical density (OD) was computed, and the cytotoxicity curves were graphed to ascertain the half-maximal inhibitory concentration (IC_{50}) values, which indicate the concentration of nanoparticles necessary to inhibit 50% of cell growth.

Molecular docking

The molecular docking was processed to evaluate the possible affinity of cellulose and selenium compounds against the NADH binding domain in human malate dehydrogenase-1. Protein data bank access was granted for the target protein with the code 7rrl. The crystallographic abnormalities were rectified by eliminating water molecules from the complex and filling in the empty valence atoms. The application of the CHARMM force fields resulted in a decline in the energy of protein structure. Therefore, the necessary arrangements for the docking procedure must be established and made. The structure of Cellulose was acquired using the Pub-Chem database. The structure was then subjected to protonation and energy reduction using the MMFF94 force field (Tosco et al. 2014). The minimized structure was prepared for docking via the ligand preparation tools. The docking process was carried out through the docking option using MOE 2014 software (Saleh et al. 2023). The receptor was immobilized, while the ligands were let to exhibit flexibility. During the refining process, each molecule was permitted to generate 20 distinct conformations with the proteins. The docking scores, which represent the affinity energy, for the most suitable poses with the active sites were recorded. Subsequently, 3D figures were created using the Discovery Studio 2016 visualizer (El Azab et al. 2023).

Isolation and determination of malate dehydrogenase (MDH-1) activity

After the treatment, the cells were harvested, washed with 0.05 M phosphate-buffered saline (PBS), and homogenized in 1.5 mL 50 mM phosphate buffer, pH 7.5 using teflon pestle homogenizer at 4 °C, then centrifuged for 15 min at 8000 rpm. MDH activity was measured in the supernatant that contains the crude enzyme according to (El-Keiy et al. 2019). Briefly, 0.1 mL homogenate was mixed with 0.85 mL NAD^+ (3.6 mmol/L), then added to 50 µL of sodium malate (500 mmol/L) to start the reaction. The activity of MDH-1 was estimated by detecting the rise in the extinction coefficient of NAD^+ at 340 nm, with an extinction coefficient of 6200 M^{-1} cm^{-1}. The activity of the enzyme was depicted as micromoles of NAD^+ (µmol/min/mg protein). An estimation of the protein content was performed using Bradford reagent (Bradford 1976).

Molecular investigations

Flow cytometric measurements

Studying cell cycles Propidium iodide (PI) was used for cell cycle analysis in accordance with the methods described by Pozarowski and Darzynkiewicz (2004). Briefly, cells with treatment were rinsed twice with PBS and then subjected to centrifugation. The aqueous component was extracted, and the cells were submerged in 500 mL of 70% ethanol that

had been chilled to −20 °C for at least 2 h. The fluid was spun at 1000 rpm for 5 min to separate the components and get rid of the ethanol. The cells that had been stuck together were washed with PBS and then mixed with 500 mL of PI labeling solution. Prior to inquiry, the cells that had been stained were kept in darkness for a period of 30–60 min at room temperature. Subsequently, they were processed using the Attune flow cytometer manufactured by Applied Bio-system in the United States.

Intracellular ROS The production of total intracellular reactive oxygen species (ROS) in cells treated with nanocellulose, nanoselenium, and the nanocomposite was assessed according to the guidelines of the ENZO ROS detection kit (ENZ-51011) (Hajnal et al. 2023). Nanocomposite, nanocellulose, and nanoselenium were added to the cells at IC_{50} concentrations. Following a brief rinse with ROS buffer, the treated cells were subjected to centrifugation at a speed of 4000 rpm for 5 min. Subsequently, the cells were treated with the fluorescent probe DCFH-DA and allowed to incubate for 30 min. The intracellular reactive oxygen species (ROS) stayed measured by quantifying the fluorescence intensity using an Accuri C6 flow cytometer with 495 nm excitation and 520 nm emissions. Nanocellulose, nanoselenium, and the nanocomposite all contributed to an increase in fluorescence intensity that was proportionate to the amount of reactive oxygen species (ROS) produced by the cells.

Quantitative real-time PCR

The subsequent information provides an approximation of the gene expression level of cytosolic malate dehydrogenase (MDH-1), together with the housekeeping gene glyceraldehyde-3-phosphate dehydrogenase (GAPDH): before adding 12.5 µL of 2X Maxima SYBR Green/ROX qPCR Master Mix and 7.5 µL of nuclease-free water, 3 µL of cDNA template (10–20 ng/µL) and 1 µL of forward primers (10 µM) and reverse primers (0.1–0.5 µM) were combined (Hanse et al. 2017). Table 1 lists the primer sequences utilized in the amplification. The completed reaction mixture was put into the Step One Plus real-time thermal cycler, and then it was run using the PCR optimum conditions for 45 cycles. Target gene quantities critical threshold (Ct) were standardized with that of the housekeeping gene via the use of a $2^{-\Delta\Delta Ct}$ method (Livak and Schmittgen 2001).

Quantitative analysis of data using statistical methods

The data were presented by utilizing three replicates from each experimental group and represented as the mean ± standard deviation (SD). One-way analysis of variance (ANOVA) was used to compare the groups in the data, and then Tukey's test was run on GraphPad Prism Software 6 (San Diego, CA). There was a statistical consequence when the chance value was less than 0.05, which is written as $P < 0.05$. The number is 3.

Table 1 Forward and reverse primer sequences

Genes	Forward primer (5′–3′)	Reverse primer (5′–3′)
MDH-1	GGACGATAAGTCTGAACCAATCA	CCAAAGACAGATCCATTTCCAATAC
GAPDH	ACCCACTCCTCCACCTTTGAC	TGTTGCTGTAGCCAAATTCGTT

Results and discussion

Nanocellulose, nanoselenium, and their nanocomposite were successfully synthesized. Nanocellulose had 24–66 nm spherical particles. Nanoselenium formed 20 nm crystalline selenium nanoparticles. The nanocomposite integrated both phases with 15–85 nm. Techniques such as FTIR, XRD, TEM, SEM, and DLS confirmed the successful synthesis and distinct properties of these nanomaterials, as our research published (El-Sheekh et al. 2024).

Assessing the toxicity of nanomaterials using cytotoxicity assays in vitro

Comparing the effects of chemotherapy Dox on the proliferation of several cell lines, including the A549 lung cancer cell line, the MCF-7 breast cancer cell line, and the WI-38 normal cell line, the cytotoxic effects of cellulose, nanocellulose, selenium, nanoselenium, and their nanocomposite were assessed using the MTT assay, as shown in Fig. 1A–D. Nanocellulose, nanoselenium, and nanocomposite show significantly lower IC_{50} values compared to cellulose, indicating enhanced cytotoxicity. The lowest IC_{50} values are observed for both nanoselenium and the nanocomposite 40 and 38 $\mu g/mL^{-1}$, respectively, on A549 (Menon and Shanmugam 2020) (Fig. 1A). Nanoselenium and nanocomposite show the lowest significant IC_{50} values 34 and 25 $\mu g/mL^{-1}$, respectively, proving that they demonstrate strong anticancer effects on breast cancer cells The MCF-7 (Barzegarparay et al. 2023; Nazir and Iqbal 2020) as (Fig. 1B). Nanoselenium and nanocomposite 117 and 187 $\mu g/mL^{-1}$, respectively, demonstrate low significant toxicity towards WI-38 cells (Abd-Rabou et al. 2020), as

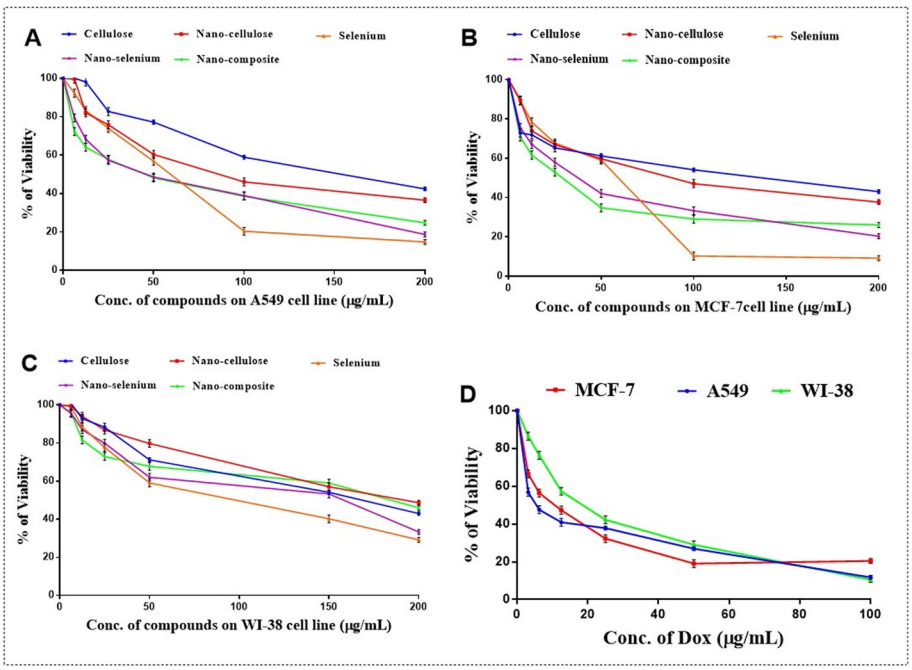

Fig. 1 The MTT assay stayed charity to assess cytotoxic possessions of cellulose, nanocellulose, selenium, nanoselenium, nanocomposite, and Dox on the viability of A549 lung cancer cell line, MCF-7 breast cancer cell line, and WI-38 normal cell line. Cells were treated for 48 h with different amounts of the previous substance

Table 2 The calculated IC_{50} of different materials on the growth of A549 lung cancer cells, MCF-7 breast cancer cells and WI-38 normal cells

IC_{50} (μg mL^{-1})			
Sample	**A549**	**MCF-7**	**WI-38**
Dox	5.899	9.041	18.12
Cellulose	145.2	130.6	157.3
Nanocellulose	90.52	86.10	193.6
Selenium	50.49	42.83	86.90
Nanoselenium	40.58	34.29	117.3
Nanocomposite	38.67	25.88	187.6

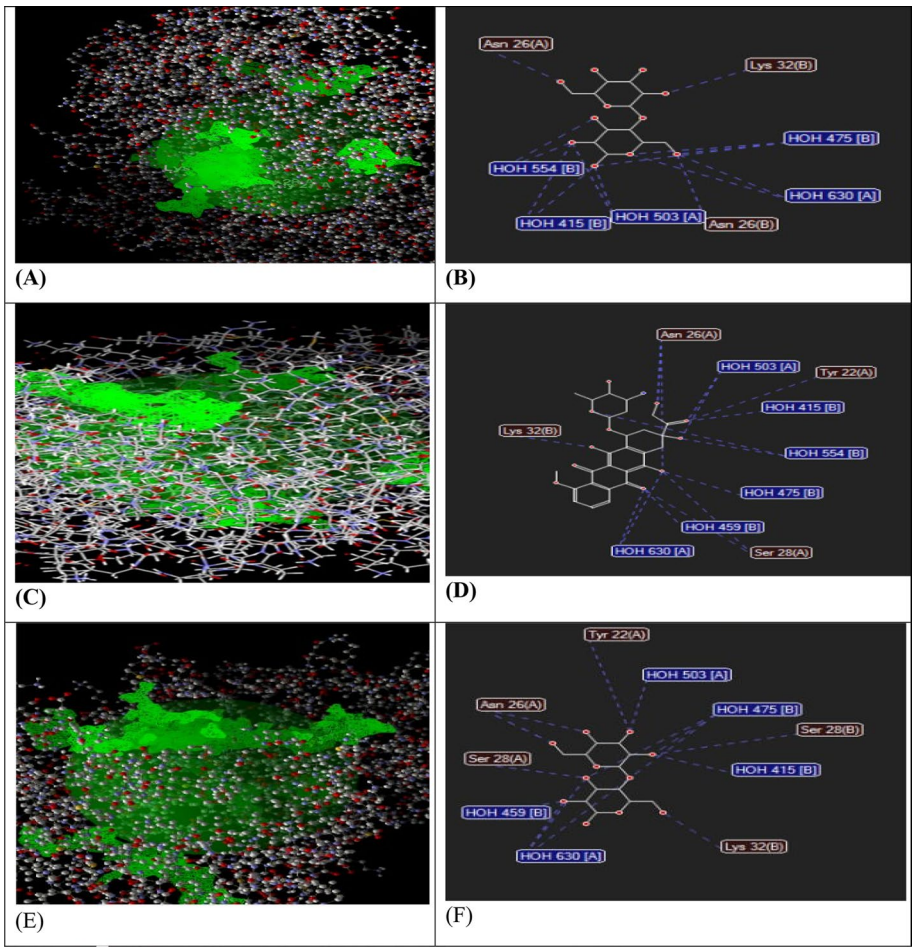

Fig. 2 The relations between cellulose, Dox and cellulose with selenium as acofactor and the active site of MDH-1. **A** 3D and **B** 2D complex enzyme ligand interaction with cellulose. **C** 3D and **D** 2D with Dox, while **E** 3D and **F** 2D of cellulose and selenium as cofactor

Fig. 1C. The cytotoxic effect of WI-38 cell line as Table 2 appears to be the most sensitive, with an IC_{50} at 8 μg/mL^{-1}, followed by A549 IC_{50} 15 μg/mL^{-1} and MCF-7 IC_{50} 25 μg/mL^{-1} (Hasanin et al. 2022). This chart serves as a reference for the cytotoxicity of a known chemotherapeutic agent, doxorubicin, across the different cell lines

(Fig. 2D). The nanocomposite and nanoselenium are highly effective against cancer cells, in particular, are very promising for breast cancer treatment due to its low IC_{50} value on MCF-7.

Molecular docking

Docking was performed to elucidate molecular interactions and docking scores between the cellulose, Dox, and cellulose with selenium as cofactor ligand molecules and the target MDH-1 protein (McCue and Finzel 2021). MDH-1 is a well-recognized, attractive therapeutic target protein for anticancer drug design. Doxorubicin (Dox) and cellulose showed the best binding affinity against the target MDH-1 protein (MDS = 8316.94 and 6125.8 kcal mol^{-1}, respectively) and inhibition constant (Ki) 114.579 with cellulose, 127.88 with Dox and (Cellulose and selenium as cofactor) is 136.98 nM. Cellulose also shows higher residue specificity (RS), indicating more precise binding to key residues (Ashraf et al. 2021) and more favorable hydrogen bonding (HB) with a value of −18.790 kcal/mol compared to Dox −8.665 kcal/mol as in Table 3. The active sites of the MDH-1 enzyme were cleared of any naturally occurring ligands. Subsequently, cellulose and Dox were curtailed into the binding site of the MDH-1 enzyme. The dimensions of the MDH-1 and cellulose binding were $x = 65.96$ Å, $y = 19.83$ Å, and $z = 181.03$ Å. The docking simulations of cellulose revealed hydrogen bond interactions with Asn 26(A), Lys 32(B), HOH 475[B], HOH 630[A], Asn 26(B), HOH 530[A], HOH 415[B], and HOH 554[B]. On the other hand, Dox interacts with Asn 26(A), HOH 503[A], Tyr 22(A), HOH 415[B], HOH 554[B], HOH 475[B], HOH 459[B], Ser 28(A), HOH 630[A], and Lys 32(B), as Fig. 2, along with other adjacent amino acid residues. Theoretically, this explains why cellulose and Dox decrease MDH-1 enzyme activity. Table 3 of the molecular model shows that docking cellulose, Dox and cellulose with selenium as cofactor to the active site of the MDH-1 enzyme resulted in the lowest energy for both compounds.

Molecular investigation

Malate dehydrogenase-1 (MDH-1) activity and gene expression in MCF-7

The untreated MCF-7 displayed a high level of MDH activity, representing the negative control (Fig. 3A). Cells treated with cellulose moderately reduced MDH-1 activity compared to the untreated control. In contrast, nanocellulose treatment significantly reduced MDH-1 activity, suggesting a potential inhibitory effect on cellular metabolism. Cells treated with selenium treatment also decreased MDH-1 activity, albeit to a reduced level than nanocellulose. Nanoselenium treatment exhibited the lowest MDH-1 activity among all groups, indicating a strong inhibitory

Table 3 The planned molecular docking factors

Factor	BE	Ki	MDS	RS	HB
Inhibitor cellulose	−67.886	114.579	6125.8	123.27	−18.790
Inhibitor Dox	−75.767	127.88	8316.94	577.39	−8.665
Inhibitor cellulose and selenium as cofactor	−81.160	136.98	5124.544	132.101	−10.227

BE binding interaction, *Ki* inhibition constant, *MDS* molecular docking score, *RS* Rerank score, *HB* hydrogen bond interaction energy

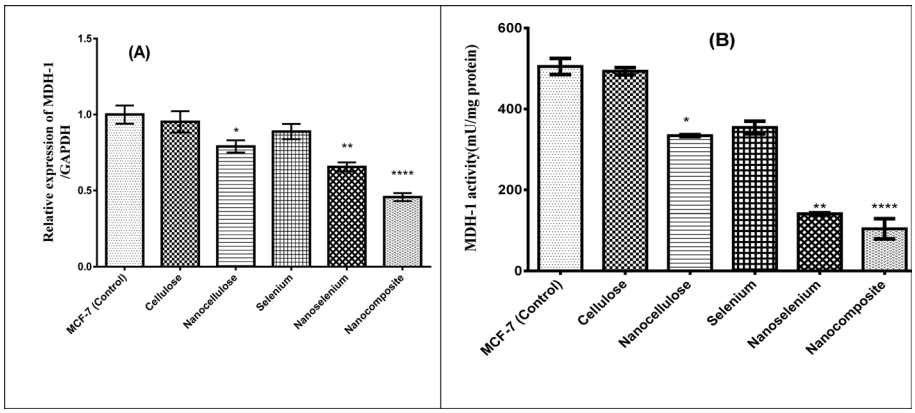

Fig. 3 **A** Activity of MDH-1 in MCF-7 cell. **B** The relative expression level of malate dehydrogenase (MDH-1) of the different groups. Data are stated as the mean ± SE

effect on MDH-1 activity (Mikhailova 2023). The current data are in agreement with Mansouri et al. (2017), who confirmed that MDH-1 has higher maximal activity in tumor tissue samples when compared with healthy tissue samples where the cell treated with nanocomposite, which combined nanocellulose and nanoselenium, also showed significantly reduced MDH-1 activity compared to the control this is due to recovery for cancer of the cells. The observed changes in MDH-1 activity relate to the potential anticancer effects of these nanoparticles, as MDH-1 is essential for cellular metabolism and the creation of energy. Reduced MDH-1 activity inhibits these activities, potentially principal to the defeat of cancer cell advance and proliferation. The confirmation of these results was achieved through the analysis of real-time PCR data, which assessed the relative mRNA expression levels of the malate dehydrogenase (MDH-1) gene in the control and treated groups. The control group exhibited significantly higher expression ($P < 0.05$) of the MDH-1 gene compared to the treated groups (Mansouri et al. 2017) (Fig. 3B). Treatment with cellulose, nanocellulose, selenium, and nanoselenium resulted in a notable down-regulation ($P < 0.05$) as the same in activity level MDH-1 mRNA expression levels compared to the untreated control group, showing that these compounds can effectively suppress the expression of the MDH-1 gene in MCF-7 cells. The nanoselenium and nanocomposite containing both nanocellulose and nanoselenium exhibited the most potent inhibition of MDH-1 mRNA expression. This observation supports that the synergistic effects observed in this change of down-regulated expression were compatible with MDH-1 activity. Nanoselenium and nanocomposite demonstrate MDH-1 enhanced anticancer activity compared to untreated and also showed the inhibition of MDH-1 in agreement with Dong et al. (2014). The molecular docking studies revealed favorable binding interactions between cellulose and the NADH binding domain of MDH-1, finding that cellulose and its derivatives may exert their anticancer effects by modulating the activity of this metabolic enzyme. The inhibition of MDH-1 mRNA expression observed in the real-time PCR data supports this hypothesis, as reduced gene expression can lead to lower levels of the enzyme and subsequent disruption of cellular metabolism.

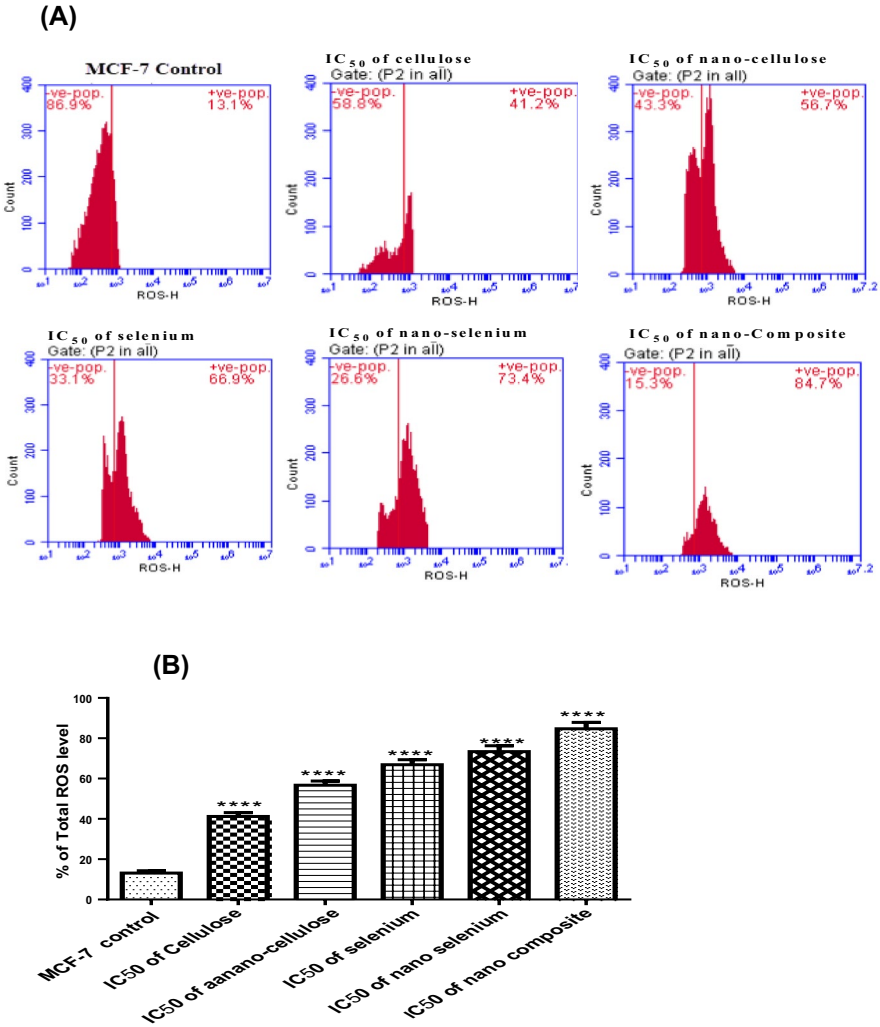

Fig. 4 **A** DCFH-DA staining sample flow cytometry of MCF-7 cells treated with IC_{50} for 48 h to measure total intracellular ROS. **B** The total ROS histogram was compared to untreated MCF-7 using one-way ANOVA, where $^{****}P < 0.0001$ for untreated cells

Flow cytometric measurement

Intracellular ROS content Figure 4 shows the results of a flow cytometric study of total intracellular ROS concentration in MCF-7 cells treated with IC_{50} using the DCFH-DA staining test. The proportion of overall reactive oxygen species (ROS) levels in MCF-7 cells treated with cellulose, nanocellulose, selenium, nanoselenium, and their nanocomposite at their respective IC_{50} values demonstrated a significant rise in apoptosis. The control group of MCF-7 cells without any treatment exhibited the highest ROS level, which is expected for cancer cells due to their increased metabolic activity. Elevated amounts of reactive oxygen species (ROS) can lead to cellular harm, reliant on the interval of ROS stress. This can trigger apoptosis, a process of programmed cell death, by controlling the expression of several proteins involved in regulating apoptosis (Trachootham et al. 2006). The ROS stress-response system is the target of a distinctive cancer therapy strategy that is even targeted to destroy cancer cells selectively (Raj et al. 2011). Cells treated with the

IC_{50} concentration of cellulose presented a significant decline in ROS levels related to the control group. This means that cellulose can potentially alleviate oxidative stress in MCF-7 cells (Mohammed et al. 2019). Treatment with the IC_{50} concentration of nano-cellulose resulted in even lower ROS levels than cellulose (You et al. 2022), this is due to its increased surface area and improved bioavailability, according to Farooq et al. (2020). The results indicate that the tested compounds, particularly the nanostructured forms (nanocellulose and nanoselenium) and their nanocomposite, had lower ROS due to the recovery for cancer in breast cancer cells MCF-7.

Cell cycle analysis Figure 5 represents the distribution of cells in different phases of the cell cycle (G0/G1, S, and G2/M) after treatment with tested compounds at their IC_{50} concentrations. The control group of MCF-7 cells exhibited a distinct distribution of cells among various phases of the cell cycle. A significant proportion of cells (55%) were found in the G2/M phase, followed by the S phase. Smaller ratios of cells were observed

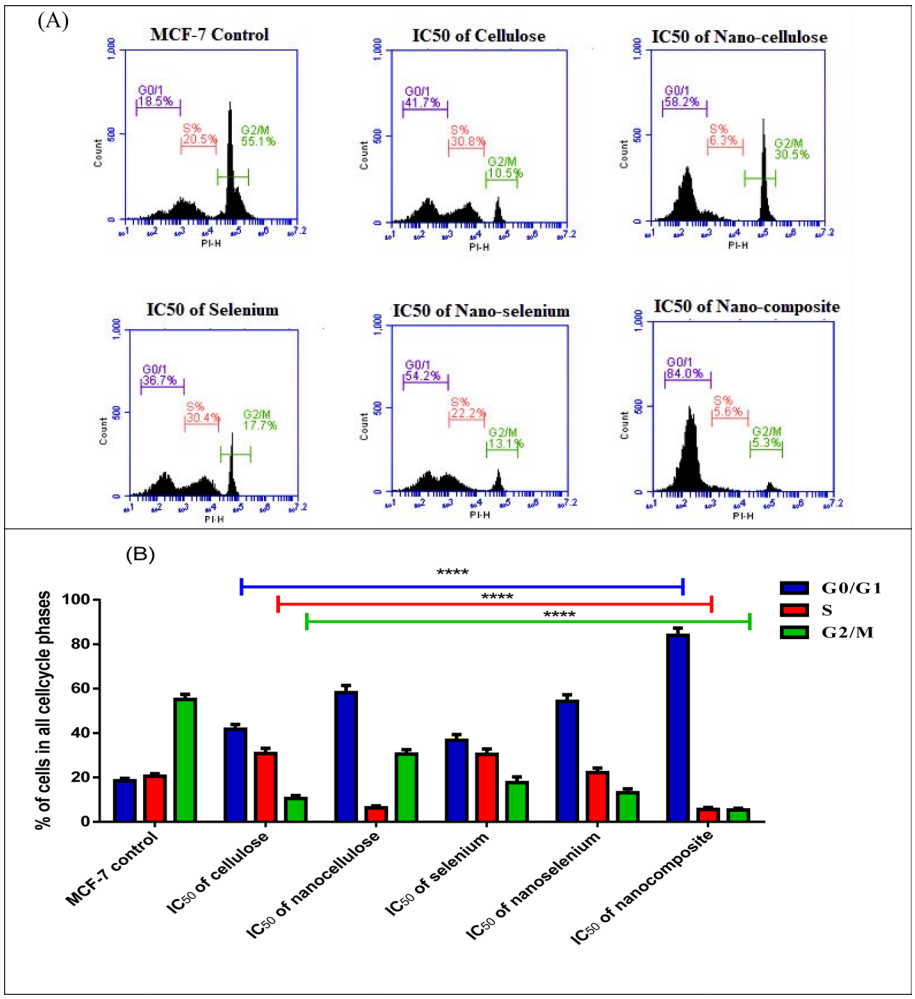

Fig. 5 **A** Cell cycle dissemination in MCF-7 breast cancer cells using flow cytometry. **B** The histogram of cell cycle was statistically analyzed using one-way ANOVA and consequences are presented as mean ± SD. $P < 0.05$ indicates significance, with * indicating significant differences from MCF-7 cells without treatment

in the G0/G1 phase. Other research conducted by Choi and Kim (2008) has revealed similar outcomes. Cells treated through the IC_{50} concentration of cellulose exhibited an increased fraction of cells in the G0/G1 phase, where cells become 41% arrested in this phase. The group that received nanocellulose showed a significant rise ($P < 0.01$) of 58% in the fraction of cell populations that were arrested in the G0/G1 phase of the cell cycle, which is reliable with the conclusions of Moghaddam et al. (2020). The results from de Miranda et al. (2014) are supported by the fact that the group that received nanocellulose had a 58% increase in the percentage of cell populations arrested in the G0/G1 phase of the cell cycle, which was statistically significant ($P < 0.01$). Cells treated with IC_{50} nanoselenium show a significant increase ($P < 0.01$) in the arrested cell by 54% in G0/G1. It is better when compared to control untreated cells (Pi et al. 2013). The nanocomposite group showed a massive increase ($P < 0.001$) with the highest fraction of cells in the G0/G1 phase among wholly treatment groups, about 84% of MCF-7 breast cancer cells. Conversely, the nanocomposite group exhibited a significant reduction ($P < 0.05$, $P < 0.01$) in the S phase. In addition, the effect on the ratio of cells in the G2/M phase was slightly less pronounced compared to the G0/G1 phase (Fig. 5B), which this result is not in agreement with He et al. (2013). The study refers to nanocomposite causing cell arrests at the S phase while this study indicates the significant high effect of the nanocomposite on MCF-7 cells at the G2/M stage. This proved that the combination of nanocellulose and nanoselenium in their nanocomposite formulation has a synergistic effect in inducing potent cell cycle arrest in the G0/G1 phase when related by the control group.

Conclusion

In this study, we have demonstrated the significant potential of nanocellulose, nanoselenium and their nanocomposite for breast cancer treatment. Our findings reveal the nanocomposite exhibits superior cytotoxicity against MCF-7 breast cancer cells compared to the conventional chemotherapeutic agent doxorubicin, suggesting its promise for nanomedicine as anticancer therapy. The nanocomposite significantly inhibits both the activity and gene expression of malate dehydrogenase (MDH-1), a key enzyme in cellular metabolism, thereby disrupting the metabolic processes essential for cancer cell growth. Furthermore, the nanocomposite shows a synergistic effect in reducing intracellular reactive oxygen species (ROS) levels, which are typically elevated in cancer cells and associated with disease progression. Our study exposes the ability of nanocomposite to induce potent cell cycle arrest in the G0/G1 phase, effectively stopping the division of MCF-7 cells. This approach used to target cancer cells, combining metabolic disruption, ROS modulation and cell cycle interference, highlights the potential of nanotechnology approaches in developing more effective and potentially less toxic cancer treatments. This research not only advances our acceptance of nanomaterial as cancer therapies but also opens new opportunities for the development of advanced treatments in the field of cancer nanotechnology.

Acknowledgements
Not applicable.

Author contributions
M.E.: reviewing and editing the manuscript. W.Y.: methodology, manuscript draft writing, E.K., T.M.: conceptualization, manuscript draft writing, and editing.

Funding
Open access funding provided by The Science, Technology & Innovation Funding Authority (STDF) in cooperation with The Egyptian Knowledge Bank (EKB).

Data availability
All data and materials are included within the manuscript.

Declarations

Ethics approval and consent to participate
Not applicable.

Consent for publication
Not applicable.

Competing interests
The authors declare no competing interests.

Received: 5 August 2024 Accepted: 12 September 2024
Published online: 03 October 2024

References

Abd-Rabou AA, Shalby AB, Ahmed HH (2019) Selenium nanoparticles induce the chemo-sensitivity of fluorouracil nanoparticles in breast and colon cancer cells. Biol Trace Elem Res 187:80–91
Abd-Rabou AA, Ahmed HH, Shalby AB (2020) Selenium overcomes doxorubicin resistance in their nano-platforms against breast and colon cancers. Biol Trace Elem Res 193:377–389
Akram M, Iqbal M, Daniyal M, Khan AU (2017) Awareness and current knowledge of breast cancer. Biol Res 50:1–23
Arnold M, Morgan E, Rumgay H, Mafra A, Singh D, Laversanne M, Vignat J, Gralow JR, Cardoso F, Siesling S (2022) Current and future burden of breast cancer: global statistics for 2020 and 2040. The Breast 66:15–23
Ashraf SA, Elkhalifa AEO, Mehmood K, Adnan M, Khan MA, Eltoum NE, Krishnan A, Baig MS (2021) Multi-targeted molecular docking, pharmacokinetics, and drug-likeness evaluation of okra-derived ligand abscisic acid targeting signaling proteins involved in the development of diabetes. Molecules 26:5957
Barzegarparay F, Najafzadehvarzi H, Pourbagher R, Parsian H, Ghoreishi SM, Mortazavi-Derazkola S (2023) Green synthesis of novel selenium nanoparticles using *Crataegus monogyna* extract (SeNPs@ CM) and investigation of its toxicity, antioxidant capacity, and anticancer activity against MCF-7 as a breast cancer cell line. Biomass Conv Bioref. https://doi.org/10.1007/s13399-023-04604-z
Biancur DE, Kimmelman AC (2018) The plasticity of pancreatic cancer metabolism in tumor progression and therapeutic resistance. Biochim Biophys Acta Rev Cancer 1870(1):67–75
Bradford MM (1976) A rapid and sensitive method for the quantitation of microgram quantities of protein utilizing the principle of protein-dye binding. Anal Biochem 72:248–254
Britt KL, Cuzick J, Phillips K-A (2020) Key steps for effective breast cancer prevention. Nat Rev Cancer 20:417–436
Chen W, Li X, Cheng H, Zhan X, Xia W (2023) Synthesis, characterization, and anticancer activity of protamine sulfate stabilized selenium nanoparticles. Food Res Int 164:112435
Choi EJ, Kim G-H (2008) Daidzein causes cell cycle arrest at the G1 and G2/M phases in human breast cancer MCF-7 and MDA-MB-453 cells. Phytomedicine 15:683–690
Chuang ST, Conklin B, Stein JB, Pan G, Lee K-B (2022) Nanotechnology-enabled immunoengineering approaches to advance therapeutic applications. Nano Converg 9:19
de Bari L, Atlante A (2018) Including the mitochondrial metabolism of L-lactate in cancer metabolic reprogramming. Cell Mol Life Sci 75:2763–2776
de Miranda JX, de Oliveira Andrade F, de Conti A, Dagli MLZ, Moreno FS, Ong TP (2014) Effects of selenium compounds on proliferation and epigenetic marks of breast cancer cells. J Trace Elem Med Biol 28:486–491
Dong S-W, Gao Z-H, Shen X-Y, XueXia H-WL (2014) Comparative proteomic analysis shows an elevation of Mdh1 associated with hepatotoxicity induced by copper nanoparticle in rats. J Integr Agric 13:1073–1081
El Azab EF, Alakilli SY, Saleh AM, Alhassan HH, Alanazi HH, Ghanem HB, Yousif SO, Alrub HA, Anber N, Elfaki EM (2023) *Actinidia deliciosa* extract as a promising supplemental agent for hepatic and renal complication-associated type 2 diabetes (in vivo and in silico-based studies). Int J Mol Sci 24:13759
El-Keiy MM, Radwan AM, Mohamed TM (2019) Cytotoxic effect of soy bean saponin against colon cancer. J Biosci Med 7:70–86
El-Sheekh MM, Yousuf WE, Kenawy E-R, Mohamed TM (2023) Biosynthesis of cellulose from *Ulva lactuca*, manufacture of nanocellulose and its application as antimicrobial polymer. Sci Rep 13:10188
El-Sheekh MM, Yousuf WE, Mohamed TM, Kenawy ER (2024) Synergistic antimicrobial action of nanocellulose, nanoselenium, and nanocomposite against pathogenic microorganisms. Int J Biol Macromol 268(2):131737
Eniafe J, Jiang S (2021) The functional roles of TCA cycle metabolites in cancer. Oncogene 40:3351–3363
Fan Z, Iqbal H, Ni J, Khan NU, Irshad S, Razzaq A, Cheng H (2024) Rationalized landscape on protein-based cancer nanomedicine: recent progress and challenges. Int J Pharm X 7:100238

Farooq A, Patoary MK, Zhang M, Mussana H, Li M, Naeem MA, Mushtaq M, Farooq A, Liu L (2020) Cellulose from sources to nanocellulose and an overview of synthesis and properties of nanocellulose/zinc oxide nanocomposite materials. Int J Biol Macromol 154:1050–1073
Grishkewich N, Mohammed N, Tang J, Tam KC (2017) Recent advances in the application of cellulose nanocrystals. Curr Opin Colloid Interface Sci 29:32–45
Hajnal A, Bogdandi N, Marokházi J, Guba D, Mikus EG (2023) Cell-type-specific determination of reactive oxygen species by flow cytometry. Andrology 11:1558–1565
Hanse EA, Ruan C, Kachman M, Wang D, Lowman XH, Kelekar A (2017) Cytosolic malate dehydrogenase activity helps support glycolysis in actively proliferating cells and cancer. Oncogene 36:3915–3924
Hasanin M, Taha NF, Abdou AR, Emara LH (2022) Green decoration of graphene oxide nano sheets with gelatin and gum Arabic for targeted delivery of doxorubicin. Biotechnol Rep 34:e00722
He N, Shi X, Zhao Y, Tian L, Wang D, Yang X (2013) Inhibitory effects and molecular mechanisms of selenium-containing tea polysaccharides on human breast cancer MCF-7 cells. J Agric Food Chem 61:579–588
Iqbal H, Razzaq A, Khan NU, Rehman SU, Webster TJ, Xiao R, Menaa F (2022) pH-responsive albumin-coated biopolymeric nanoparticles with lapatinab for targeted breast cancer therapy. Biomater Adv 139:213039
Khalil HA, Yahya EB, Jummaat F, Adnan A, Olaiya N, Rizal S, Abdullah C, Pasquini D, Thomas S (2023) Biopolymers based aerogels: a review on revolutionary solutions for smart therapeutics delivery. Prog Mater Sci 131:101014
Koju N, Qin Z-H, Sheng R (2022) Reduced nicotinamide adenine dinucleotide phosphate in redox balance and diseases: a friend or foe? Acta Pharmacol Sin 43:1889–1904
Li T, Chen C, Brozena AH, Zhu J, Xu L, Driemeier C, Dai J, Rojas OJ, Isogai A, Wågberg L (2021) Developing fibrillated cellulose as a sustainable technological material. Nature 590:47–56
Livak KJ, Schmittgen TD (2001) Analysis of relative gene expression data using real-time quantitative PCR and the 2−ΔΔCT method. Methods 25(4):402–408
Maghsoudnia N, Eftekhari RB, Sohi AN, Zamzami A, Dorkoosh FA (2020) Application of nano-based systems for drug delivery and targeting: a review. J Nanopart Res 22:1–41
Mansouri S, Shahriari A, Kalantar H, Moini Zanjani T, Haghi Karamallah M (2017) Role of malate dehydrogenase in facilitating lactate dehydrogenase to support the glycolysis pathway in tumors. Biomed Rep 6:463–467
Maurya S, Tiwari S, Mothukuri MC, Tangeda CM, Nandigam RNS, Addagiri DC (2023) A review on recent developments in cancer detection using machine learning and deep learning models. Biomed Signal Process Control 80:104398
McCue WM, Finzel BC (2021) Structural characterization of the human cytosolic malate dehydrogenase I. ACS Omega 7:207–214
Menon S, Shanmugam V (2020) Cytotoxicity analysis of biosynthesized selenium nanoparticles towards A549 lung cancer cell line. J Inorg Organomet Polym Mater 30:1852–1864
Mikhailova EO (2023) Selenium nanoparticles: green synthesis and biomedical application. Molecules 28:8125
Moghaddam SV, Abedi F, Alizadeh E, Baradaran B, Annabi N, Akbarzadeh A, Davaran S (2020) Lysine-embedded cellulose-based nanosystem for efficient dual-delivery of chemotherapeutics in combination cancer therapy. Carbohyd Polym 250:116861
Mohammed HA, Al-Omar MS, El-Readi MZ, Alhowail AH, Aldubayan MA, Abdellatif AA (2019) Formulation of ethyl cellulose microparticles incorporated pheophytin a isolated from *Suaeda vermiculata* for antioxidant and cytotoxic activities. Molecules 24:1501
Mukherjee S, Malik P, Mukherjee TK (2023) Common reagents and medium for mammalian cell culture. Practical approach to mammalian cell and organ culture. Springer, Singapore, pp 137–185
Nazir F, Iqbal M (2020) Synthesis, characterization and cytotoxicity studies of aminated microcrystalline cellulose derivatives against melanoma and breast cancer cell lines. Polymers 12:2634
Pandey S, Awasthee N, Shekher A, Rai LC, Gupta SC, Dubey SK (2021) Biogenic synthesis and characterization of selenium nanoparticles and their applications with special reference to antibacterial, antioxidant, anticancer and photocatalytic activity. Bioprocess Biosyst Eng 44:2679–2696
Peng Y, Liu H, Liu J, Long J (2022) Post-translational modifications on mitochondrial metabolic enzymes in cancer. Free Radical Biol Med 179:11–23
Pi J, Jin H, Liu R, Song B, Wu Q, Liu L, Jiang J, Yang F, Cai H, Cai J (2013) Pathway of cytotoxicity induced by folic acid modified selenium nanoparticles in MCF-7 cells. Appl Microbiol Biotechnol 97:1051–1062
Pozarowski P, Darzynkiewicz Z (2004) Analysis of cell cycle by flow cytometry. Methods Mol Biol 281:301–311
Raj L, Ide T, Gurkar AU, Foley M, Schenone M, Li X, Tolliday NJ, Golub TR, Carr SA, Shamji AF (2011) Selective killing of cancer cells by a small molecule targeting the stress response to ROS. Nature 475:231–234
Reshmy R, Philip E, Madhavan A, Arun K, Binod P, Pugazhendhi A, Awasthi MK, Gnansounou E, Pandey A, Sindhu R (2021) Promising eco-friendly biomaterials for future biomedicine: cleaner production and applications of nanocellulose. Environ Technol Innov 24:101855
Saleh AM, Mahdy HA, El-Zahabi MA, Mehany AB, Khalifa MM, Eissa IH (2023) Design, synthesis, in silico studies, and biological evaluation of novel pyrimidine-5-carbonitrile derivatives as potential anti-proliferative agents, VEGFR-2 inhibitors and apoptotic inducers. RSC Adv 13:22122–22147
Sinha A, Simnani FZ, Singh D, Nandi A, Choudhury A, Patel P, Jha E, Kaushik NK, Mishra YK, Panda PK (2022) The translational paradigm of nanobiomaterials: biological chemistry to modern applications. Mater Today Bio 17:100463
Sk UH, RoyMahapatra D, Bhattacharya S (2022) Selenium nanoparticle in the management of oxidative stress during cancer chemotherapy. In: Chakraborti S (ed) Handbook of oxidative stress in cancer: therapeutic aspects. Springer, Singapore, pp 1–32
Tosco P, Stiefl N, Landrum G (2014) Bringing the MMFF force field to the RDKit: implementation and validation. J Cheminf 6:1–4
Trachootham D, Zhou Y, Zhang H, Demizu Y, Chen Z, Pelicano H, Chiao PJ, Achanta G, Arlinghaus RB, Liu J (2006) Selective killing of oncogenically transformed cells through a ROS-mediated mechanism by β-phenylethyl isothiocyanate. Cancer Cell 10:241–252

Wahlström N, Edlund U, Pavia H, Toth G, Jaworski A, Pell AJ, Choong FX, Shirani H, Nilsson KPR, Richter-Dahlfors A (2020) Cellulose from the green macroalgae *Ulva lactuca*: isolation, characterization, optotracing, and production of cellulose nanofibrils. Cellulose 27:3707–3725

Wang Y, Iqbal H, Ur-Rehman U, Zhai L, Yuan Z, Razzaq A, Xiao R (2023) Albumin-based nanodevices for breast cancer diagnosis and therapy. J Drug Deliv Sci Technol 79:104072

Wang R, Zhang L, Razzaq A, Khan NU, Alfaifi MY, Elbehairi SEI, Shati AA, Iqbal H, Ni J (2024) Albumin-coated green-synthesized zinc oxide nanoflowers inhibit skin melanoma cells growth via intra-cellular oxidative stress. Int J Biol Macromol 263(1):130694

You C, Ning L, Zhang Z, Wu H, Qu Q, Wang F, Xiong R, Huang C (2022) Toxic reactive oxygen species enhanced chemodynamic therapy by copper metal-nanocellulose based nanocatalysts. Carbohyd Polym 289:119432

Yusefi M, Soon ML-K, Teow S-Y, Monchouguy EI, Neerooa BNHM, Izadiyan Z, Jahangirian H, Rafiee-Moghaddam R, Webster TJ, Shameli K (2022) Fabrication of cellulose nanocrystals as potential anticancer drug delivery systems for colorectal cancer treatment. Int J Biol Macromol 199:372–385

Zambonino MC, Quizhpe EM, Mouheb L, Rahman A, Agathos SN, Dahoumane SA (2023) Biogenic selenium nanoparticles in biomedical sciences: properties, current trends, novel opportunities and emerging challenges in theranostic nanomedicine. Nanomaterials 13:424

Zhang J, Zhan P, Tian H (2021) Recent updates in the polysaccharides-based nano-biocarriers for drugs delivery and its application in diseases treatment: a review. Int J Biol Macromol 182:115–128

Zhong L, Li Y, Xiong L, Wang W, Wu M, Yuan T, Yang W, Tian C, Miao Z, Wang T (2021) Small molecules in targeted cancer therapy: advances, challenges, and future perspectives. Signal Transduct Target Ther 6:1–48

Publisher's Note